A R C H I V E S O F M E T A L L U R G Y A N D M A T E R I A L S
Volume 60 2015 Issue 3
DOI: 10.1515/amm-2015-0339

M. NADOLSKI*#, G. GOLAŃSKI**, J. KLIMAS*, M. SZOTA**, J. SZYMAŃSKI***

MICROSTRUCTURE AND FUNCTIONAL PROPERTIES OF PROSTHETIC COBALT ALLOYS CoCrW

MIKROSTRUKTURA I WŁAŚCIWOŚCI UŻYTKOWE PROTETYCZNYCH STOPÓW KOBALTU CoCrW

The material subject to investigation was two commercial alloys of cobalt CoCrW (No. 27 and 28) used in prosthodontics. The scope of research included performing an analysis of microstructure and functional properties (microhardness, wear resistance and corrosion resistance), as well as dilatometric tests. The examined alloys were characterized by diverse properties, which was considerably influenced by the morphology of precipitates in these materials. Alloy No. 27 has a higher corrosion resistance, whereas alloy No. 28 shows higher microhardness, better wear resistance and higher coefficient of linear expansion. Lower value of the expansion coefficient indicates less probability of initiation of a crack in the facing ceramic material.

Keywords: cobalt alloy, microstructure, properties

Badaniu poddano dwa komercyjne stopy kobaltu CoCrW (nr 27 i 28) stosowane w protetyce stomatologicznej. Zakres badań obejmował przeprowadzenie analizy mikrostrukturalnej, właściwości użytkowych (mikrotwardość, odporność na ścieranie i odporność korozyjna) oraz badania dylatometryczne. Badane stopy charakteryzowały się zróżnicowanymi właściwościami na co zasadniczy wpływ miała morfologia wydzieleń w tych materiałach. Stop nr 27 posiada wyższą odporność korozyjną natomiast stop nr 28 wykazuje: wyższą mikrotwardość, lepszą odporność na ścieranie oraz niższy współczynnik rozszerzalności liniowej. Niższa wartość współczynnika rozszerzalności liniowej wskazuje na mniejsze prawdopodobieństwo inicjacji pęknięcia licującego materiału ceramicznego.

1. Introduction

For many years, the casting technologies have been the basic method for manufacturing metal frame dentures. These technologies still create problems at the stage of both manufacturing and use. Many researchers in their works evaluated the quality of casts and the possibility of damage occurrence in dentures [1-6]. The development of Computer Aided Design/Computer Aided Manufacturing (CAD/CAM) methods, that can be currently observed, meets the demand for thin-walled elements mapping the anatomy of oral cavity and ensuring the repeatability of prosthetic works [7-9]. Along with a change in the manufacturing method, also the procedures have changed, beginning with impression taking, through the scanning of the obtained models and their processing with graphics software, to milling and sintering of repeatedly coated ceramic layers imitating teeth in terms of material and colour. The specified stages of CAD/CAM procedures, though, concern the works prepared for ceramic coatings of CoCr alloys and with the raw material prepared using metal powders.

In spite of the limitation to 6, 7 stages of performing works according to CAD/CAM, still technological problems remain. They result from the requirements set for biomaterials and from the cooperation of materials (metal-ceramics). Within the scope of biocompatibility, prosthetic alloys should not cause allergy or contain toxic substances. Moreover, they should be resistant to corrosion and loss of lustre in the environment of oral cavity [10,11]. At the same time, they should be relatively cheap and easily worked in mechanical treatment. Thus in practice, nickel-free alloys of cobalt are used. They fulfill the above-mentioned requirements and are used in the manufacturing of frames of removable partial dentures and ceramic-metal fillings [12]. With regard to the way of applying ceramics, the multistage cycle of heating up and cooling, these alloys should be characterized by the thermal expansion coefficient possibly similar to that of ceramic material. Whereas hardness of CoCr alloys designed for CAM/CAD works is significant in terms of the selection of sufficiently rigid CNC milling machine, since not all of the milling machines can work on materials of higher hardness. In the case of too soft alloys

* CZESTOCHOWA UNIVERSITY OF TECHNOLOGY, DEPARTMENT OF FOUNDRY, 19 ARMII KRAJOWEJ AV., 42-200 CZĘSTOCHOWA, POLAND
** CZESTOCHOWA UNIVERSITY OF TECHNOLOGY, INSTITUTE OF MATERIALS ENGINEERING, 19 ARMII KRAJOWEJ AV., 42-200 CZĘSTOCHOWA, POLAND
*** DEPARTMENT OF NORMAL AND CLINICAL ANATOMY, INTERFACULTY CHAIR OF ANATOMY AND HISTOLOGY, MEDICAL UNIVERSITY OF LODZ
# Corresponding author: nadolski@wip.pcz.pl

for works using the maximum work field, deformations of these alloys can occur. Hardness is at the same time a feature that determines the easiness of finishing a work and its resistance to scratch when being in use [12].

2. Material and methodology of research

The material under investigation was two commercial prosthetic alloys of cobalt designated as 27 and 28. Chemical composition of the examined material is presented in table 1.

TABLE 1

Chemical composition of the examined cobalt alloys*, % mass

No. of alloy	Co	Cr	Si	W	Other
27	62,23	27,57	1,50	8,33	< 1 (Mn, Fe, C)
28	63,00	24,00	1,33	8,00	Mo, Nb, C

*- chemical composition according to Manufacturer's data

Test samples for research were taken from a disk with an external diameter of 98 mm and thickness of 10 and 12 mm - material No. 27 and 28, respectively.

Observation and record of microstructure images was performed using an optical microscope Axiovert 25 (OM) and scanning electron microscope Joel JSM 6610LV (SEM), on metallographic specimens, electroetched. The measurement of microhardness with Vickers method was carried out using hardness testing machine Future-Tech FV-700, with the indenter load of 0.5 kG (4.903 N).

Dilatometric tests were performed with the use of an automatic dilatometer DA-3. Test pieces of around 32 mm length and diameter of 4 mm were heated for 1 hour at the heat-up rate of 16.6°C/min, and next they were blast cooled at the cooling rate maintained on the level of 16.6°C/min. The assumed cycle of heating/cooling is consistent with the process of sintering of the applied prosthetic porcelain.

Tribological tests were performed with the use of T-05 tester at the load of 397,5 g. A test in the relation of roller–block was carried out in the time of 120 minutes for both test pieces. The speed of rotation of the roller in both cases amounted to 546 rpm. The measurements of mass were made on a scales RadWag 40/160/C/1, after cleaning the test samples with acetone.

To determine the resistance to corrosion of materials designed for implants, the tests of corrosion resistance in the Ringer's solution at the temperature of 37°C were performed.

The composition of the solution was as follows: 0.39 g of potassium chloride; 8.6 g of sodium chloride; 0.48 g of calcium chloride in 1 dm^3 of solution. Electrochemical measurements were taken using an AMEL potentiostat, model 7050, digital controlled by a PC equipped with Juniorassist software, in a three-electrode system. A calomel electrode (NEK) was the reference electrode, whereas a platinum wire was the auxiliary electrode, and the examined test pieces constituted a working electrode. The potential set during the measurements was being changed from cathodal values towards anodal values, ranging from -2.0V to 5.0 V against the NEK. For the analysis of corrosion resistance, the most representative polarization curves were selected.

The polarization curves were a basis for determining the parameters that qualify the liability of the material to corrosion: corrosion potential $E_{corr.}$, corrosion current density $I_{corr.}$, resistance of polarization R_p.

The X-ray diffraction studies were performed using a diffractometer SEIFFERT XRD 3003 T-T, with the use of cobalt lamp radiation $\lambda = 0.17902$ nm. Parameters of the studies were as follows: angle step $\Delta 2\theta = 0.02^o$, calculation time $\tau = 5 \div 10$ s. The angle measuring range was $2\theta = 30 \div 100^o$.

3. Results of research and their analysis

3.1. Microstructural tests

The microstructure of the investigated cobalt alloys was a dendritic microstructure with numerous precipitates arranged on the boundaries of grains and within interdendritic areas (Figs. 1, 3). Observed microstructures of cobalt alloys are typical for this group of casting materials. On the boundaries of grains in these alloys, $M_{23}C_6$ carbides were observed [13, 14]. The examined alloys, however, were different in the morphology of eutectic precipitates. An example of the morphology of precipitates is presented in Figs. 2 and 4.

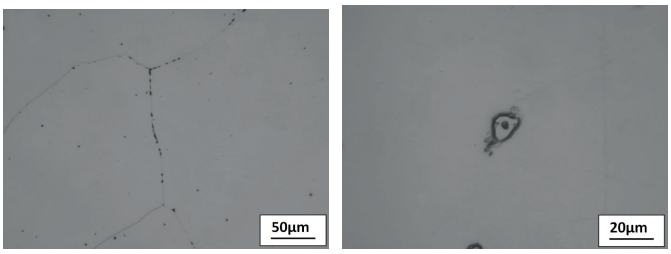

Fig. 1. Microstructure of alloy No. 27

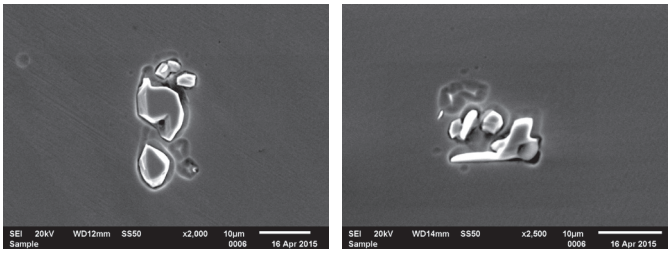

Fig. 2. Morphology of precipitates in alloy No. 27

The only precipitates observed in alloy No. 27 were similar in morphology to $M_{23}C_6$ carbides (Figs. 1, 2). These precipitates were observed on the boundaries of grains, as well as inside cobalt austenite grains. In casting alloys of cobalt, the $M_{23}C_6$ carbides precipitate as the main phase already during the solidification process [13, 15]. In the examined alloy, these carbides had a compound chemical composition – they were rich in chromium and tungsten (Fig. 5). In the case of alloy No. 28, apart from the $M_{23}C_6$ carbides precipitated on the boundaries of grains, numerous carbide eutectics were observed inside the grains (Fig. 3). Eutectics in this alloy were similar in morphology to "pearlitic" colonies (Fig. 4).

"Pearlitic" colonies in such a type of alloys, usually consist of $M_{23}C_6$ carbides, σ phase, and cobalt austenite [16]. The presence of niobium in the chemical composition of alloy No. 28 also indicates the possibility of the occurrence of MC-type precipitates in the microstructure of this material.

The investigated materials also differed in the size of cobalt austenite grain. In alloy No. 27, the grain was fine, whilst in alloy No. 28, it was bigger. The above implies different cooling rates of the examined alloys at the stage of their manufacturing. Similar observations about the influence of cooling rate on the morphology of precipitates and the grain size are presented in the work [15].

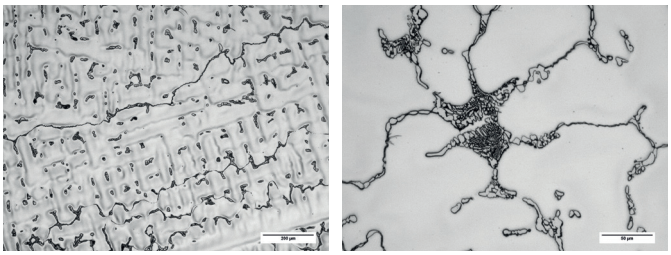

Fig. 3. Microstructure of alloy No. 28

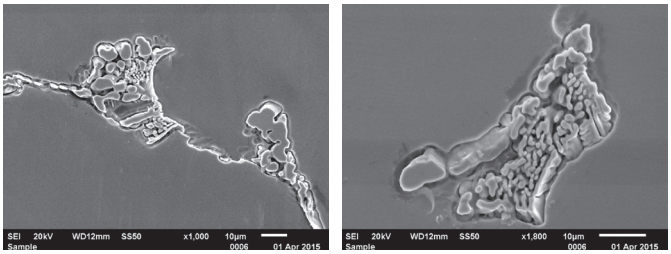

Fig. 4. Morphology of precipitates in alloy No. 28

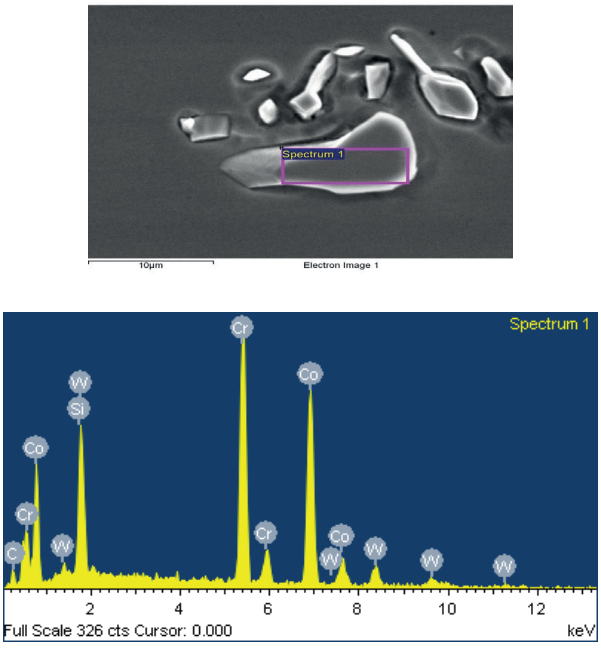

Fig. 5. Spectrum of characteristic X-radiation of precipitate in alloy No. 27

4. X-ray diffraction analysis

For the identification of the main phases present in the examined alloys, their X-ray diffraction analysis was performed. Obtained results in the form of X – ray diffraction are presented in Figs. 6 and 7.

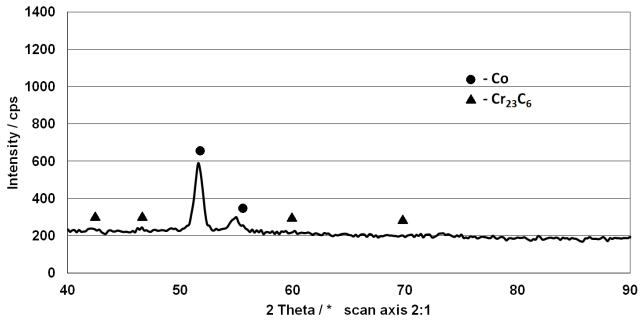

Fig. 6. X- ray diffraction of alloy No. 27

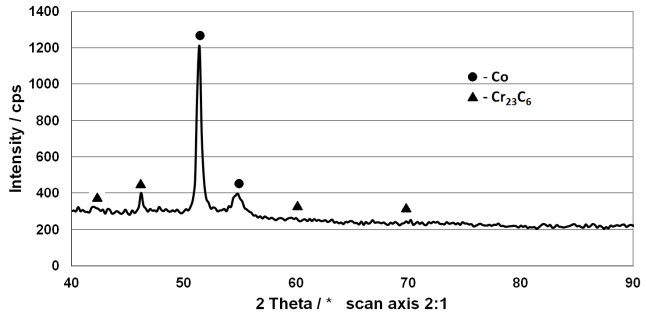

Fig. 7. X- ray diffraction of alloy No. 28

Performed X-ray diffraction quantitative analysis of phases in the CoCrW alloys proved the occurrence of two main phases: cobalt matrix (Co) and $Cr_{23}C_6$ carbides. Greater intensity of the diffraction maximum coming from $M_{23}C_6$ carbides in alloy No. 28, compared to alloy No. 27, indicates their greater amount in alloy No. 28.

5. Measurement of microhardness and tribological tests

The measurement of microhardness taken on the cross-section of CoCrW alloys showed that the microhardness of material No. 27 was in the range of 248 ÷ 307 HV0.5, whereas for material No. 28, it ranged between 290 ÷ 323 HV0.5. Higher microhardness of alloy No. 28 surely results from a relatively greater amount of precipitates in the matrix and the presence of σ-phase precipitates and probably the MC-type carbides in the microstructure. Higher microhardness of alloy No. 28 is reflected in higher wear resistance of this material in comparison with alloy No. 27. After wear testing, the mass decrement noted for alloy No. 28 amounted to 0.113%, whereas for alloy No. 27 – 0.382%. It confirms the commonly accepted dependency that wear resistance of cobalt alloys is directly dependent on their hardness.

6. Electrochemical tests results

On the basis of the registered potentiokinetic curves (Fig. 8), corrosion resistance of the examined materials in Ringer's solution was compared. According to the course of polarization curves, material No. 27 in the examined environment shows the corrosion potential of about –0.605V against NEK (see Table 2). For alloy No. 28, however, a shift of the corrosion potential towards positive values can be noticed, to the value of $E_{corr.}$ = –0.198V against NEK.

TABLE. 2
Results of electrochemical measurements of Co alloys, determined on the basis of registered potentiokinetic curves

Alloy	$E_{corr.}$ against NEK V	$I_{corr.}$ mA*mm $^{-2}$	*Rp* mΩ mm^2
27	-0.605	0.0085	637.52
28	-0.198	0.0397	122.53

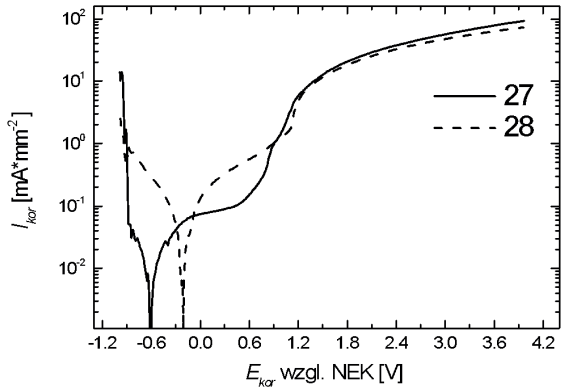

Fig. 8. Polarization curves registered for investigated materials

On the basis of the analysis of polarization curves registered for both materials (Fig. 8), in the case of material 27, a decrease in the values of corrosion currents, almost by an order of magnitude, is observed in comparison with material 28. The course of potentiokinetic curves indicates that the examined materials are subject to passivation, which is connected with the development of a protective layer that causes the effect of a decrease in the current values within the active scope. At the potential of around 0.6V against NEK for material 27, and 1.2V against NEK for material 28, there is a rapid growth of current values, which indicates a reconstruction of the passive layer and a loss of protective properties.

The resistance of material in the examined corrosive conditions can also be influenced by the value of resistance of polarization, determined on the basis of polarization curves. Fig. 9. presents the value of polarization resistance for the investigated alloys. According to the Stern-Hoar equation, in the range of potentials insignificantly different from the corrosion potential (± 20mV), the density of external current is a linear function of potential. The inclination of a straight line ΔE=f(Δi) is a measure of polarization resistance.

The determined values of Rp show that material No. 27 is characterized by higher resistance to corrosion in the examined conditions (Rp= 637.52 mΩ mm^2).

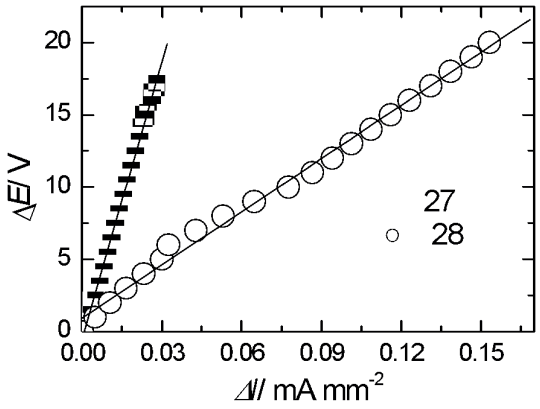

Fig. 9. Change in values of external current as function of impressed voltage (in the range of $E_{corr.}$ + ΔE) for analyzed materials, based on potentiokinetic curves illustrated in Fig. 8

7. Dilatometric measurements

On the basis of data received from the dilatometric measurements, the curves of dimensional changes were obtained, and presented as a function of temperature in Fig. 10. The course of expansion of materials No. 27 and 28 in the range of temperatures of measurement is of linear character and does not show any polymorphic changes running. It is, however, different in terms of the thermal expansion coefficient α, according to Table 3. For both materials, the change of coefficient α was recorded during heating in the temperature range of 600-1000°C. The curves of cooling in the temperature range of 1000-270°C are characterized by a linear course.

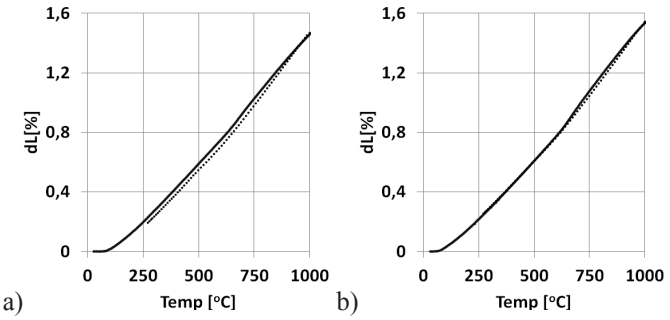

Fig. 10. Dilatometric curve of material heating No.: a) 27, b) 28

Comparing the values of final length of the test pieces for the temperature of 260°C, it was observed that the size change for material No. 27 amounted to *dl* = 0.20%, and for material No. 28 to *dl* = 0.01%. Higher gain in length of the test piece from material No. 27 can result from matrix enrichment in the atoms of elements that are included in the composition of $M_{23}C_6$ carbides. Such a type of carbide is subject to complete solution at the temperature of around 1040°C.

TABLE 3

Determined values of linear expansion coefficients α

Range of temperatures	$\alpha \times 10^{-6}\ K^{-1}$	
	27	**28**
30-600	15.48	13.71
600-1000	14.17	13.17

8. Summary

Two CoCrW alloys used in prosthodontics were subject to investigation. Performed research has shown that the analyzed alloys, in spite of their similar chemical composition, are characterized by diverse functional properties. The above is influenced by a diverse morphology of precipitates observed in the examined alloys. Alloy No. 27 is characterized by better resistance to corrosion, whereas alloy No. 28 shows higher microhardness and wear resistance. Moreover, alloy No. 28 has a lower value of linear expansion coefficient. Lower value of this coefficient for alloy No. 28 indicates less probability of initiation of a crack in the facing ceramic material.

REFERENCES

[1] I. Peter, M. Rosso, A. Toppi, I. Dan, B. Ghiban, Arch, Mat. Sci. Engi. **61**, 62 (2013),

[2] L. Reclaru, H. Lüthy, P.Y. Eschler, A. Blatter, O. Loeffel, M.H Zurcher, Euro. Cel. Mate. **7**, 51 (2004),

[3] R. Prabhu, K.R. Geetha Prabhu, T. Ilango, Jour. Clin. Diag. Res. **5(8)**, 1682 (2011),

[4] L. Reinmann, L.A. Dobrzański, Arch, Mat. Sci. Engi. **60**, 5 (2013),

[5] L.A. Dobrzański, L. Reinmann, Jour. Achie. Mate. Manu. Engi. **49**,193 (2011),

[6] Z. Komorek, S. Jóźwiak, M. Kuchta, Arch. Odle. **6**, 279 (2006),

[7] S.W. Majewski, Prot. Stom. **7**, 124 (2007),

[8] M. Gładkowska, P. Montefka, P. Okoński,, Prot. Stom. **8**, 105 (2008),

[9] F. Noack, Inter. Jour. Dental Tech. **13**, 2 (2012),

[10] A. Łukaszczyk, J. Augustyn-Pieniążek, Arch. Met. Mat., **60**, 523 (2015),

[11] D. Klimecka-Tatar, K. Radomska , G. Pawłowska, Jour. Balk. Tribol. Assoc. **21**, 204 (2015),

[12] K. Beer-Lech, M. Szala, P. Piskorska, Ł. Majewski, Badania lejności i twardości stomatologicznego stopu odlewniczego na osnowie kobaltu, in Materials Engineering - Selected issues from materials engineering (2013),

[13] L. E. Ramirez, M. Castro, M. Mendez, J. Lacaze, M. Herrera, G. Lesoult, Sc. Mater., **47**, 811 (2002)

[14] J. Augustyn – Pieniążek, A. Łukaszczyk, R. Zapała, Arch. Metal. Mater. **58**, 1281 (2013),

[15] Sh. Zangeneh, H. R. Lashagari, A. Roshani, Mater. Design **37**, 292 (2012),

[16] J. V. Giacchi, C. N. Morando, O. Fornaro, H. A. Palacio, Mater. Charact., **62**, 53 (2011).

Received: 20 March 2015.